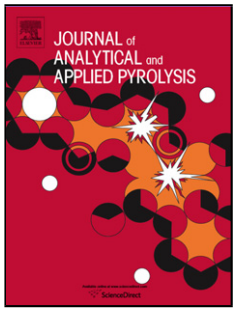

Title: Molecular characterization of the thermally labile fraction of biochar by hydropyrolysis and pyrolysis-GC/MS

Author: Alessandro G. Rombolà Daniele Fabbri Will Meredith Colin E. Snape Alba Dieguez-Alonso

PII: S0165-2370(16)30137-1
DOI: http://dx.doi.org/doi:10.1016/j.jaap.2016.08.003
Reference: JAAP 3789

To appear in: *J. Anal. Appl. Pyrolysis*

Received date: 10-3-2016
Revised date: 15-7-2016
Accepted date: 4-8-2016

Please cite this article as: Alessandro G.Rombolà, Daniele Fabbri, Will Meredith, Colin E.Snape, Alba Dieguez-Alonso, Molecular characterization of the thermally labile fraction of biochar by hydropyrolysis and pyrolysis-GC/MS, Journal of Analytical and Applied Pyrolysis http://dx.doi.org/10.1016/j.jaap.2016.08.003

<AT>Molecular characterization of the thermally labile fraction of biochar by hydropyrolysis and pyrolysis-GC/MS

<AU>Alessandro G. Rombolà[a*], Daniele Fabbri[a], Will Meredith[b], Colin E. Snape[b], Alba Dieguez-Alonso[c]
<AU>

<AFF>[a]Department of Chemistry ``Giacomo Ciamician", C.I.R.I. Energia Ambiente and C.I.R.S.A., Università di Bologna, Ravenna Campus, Via S. Alberto 163, 48123, Ravenna, Italy
<AFF>[b]Department of Chemical and Environmental Engineering, University of Nottingham, Nottingham NG7 2RD, United Kingdom, UK
<AFF>[c]Institute of Energy Engineering, Technische Universität Berlin, Fasanenstrasse 89, 10623 Berlin, Germany

<ABS-HEAD>Highlights► Consistent and complementary data from Py and HyPy GC-MS of six biochars. ► BC_{HyPy} and Py-GC-MS strongly correlated with charring degree H/C. ► HyPy semi-labile 2-7 ring PAHs more abundant than extractable PAHs. ► HyPy semi-labile PAHs more abundant in less charred biochars. ► Methylated/parent PAH ratios from HyPy and Py-GC-MS showed similar trends.

<ABS-HEAD>Abstract

<ABS-P>Agroenvironmental benefits and limitations of biochar in soil applications require a full understanding of the stability and fate of the various carbon fractions. Analytical hydropyrolysis (HyPy) enables the determination of the stable black carbon (BC_{HyPy}) and thermally labile (semi-labile; non-BC_{HyPy}) fractions in biochar and soil samples. The non-BC_{HyPy} fraction can be analysed at a molecular level by gas chromatography-mass spectrometry (GC-MS). In the present study, HyPy was applied to the characterisation of biochars produced from pine wood, beech wood and corn digestate with the same pyrolysis unit at low (340-400 °C) and high (600 °C) temperatures. Results were compared with those from Py-GC-MS. HyPy provided consistent information concerning the thermal stability of biochar samples, with BC_{HyPy} levels related with the relative abundance of the charred fraction estimated by Py-GC-MS and the hydrogen/carbon (H/C) ratios. The non-BC_{HyPy} fractions were featured by the presence of polycyclic aromatic hydrocarbons (PAHs) from two to seven rings, including alkylated derivatives up to C_4. Partially hydrogenated PAHs were also detected. The yields of non-BC_{HyPy} were higher for those biochars produced at lower temperatures and always more abundant than the levels of solvent-extractable PAHs. The methylated/parent PAH ratios from HyPy and Py-GC-MS exhibited lower values for the most charred biochar. The observed differences in the abundance of the stable fraction and the molecular chemistry of the semi-labile fraction can be usefully utilised to drive the process conditions to the desired properties of the resulting biochars and to predict the impact of

biochar amendment to soil organic pools. The concentrations of priority PAHs in the semi-labile fraction was evaluated in the mg g^{-1} level suggesting that it could be an important fraction of the polyaromatic carbon pool in soil.

<KWD>Keywords: Biochar; Hydropyrolysis; Py-GC-MS; Labile fraction; Polyaromatic

<H1>1. Introduction

Biochar is the carbonaceous solid formed by the pyrolysis of biomass which attracts research interest due to its potential value for long-term carbon sequestration. The addition of biochar to soil has been proposed as a strategy that not only sequesters carbon in soils but also mitigates different environmental issues. Research has demonstrated that biochar has considerable potential as a sustainable tool for carbon sequestration, soil amelioration, greenhouse gas emissions reduction and fertilizer runoff reduction, as well as waste management [1].

A key requirement for the use of biochar as tool for agroenvironmental management is that the carbon in the biochar is stable, meaning that a substantial fraction of the carbon sequestered is not re-mineralized on at least centennial timescales [2,3]. However, a variable component of the carbon in many biochars is degradable on annual to decadal timescales and hence, only a proportion of total carbon in biochar provides long-term carbon sequestration [4,5,6]. In fact, an increasing number of studies suggest that biochars in the environment are subject to biological, physical and chemical action, and that their chemical constitutions progressively change [7,8]. Moreover, the labile fraction, which evolves in the short-term during its storage in soil, can influence the soil microbial community structure [9], and therefore affect the functioning of the soil [10]. Biochar application on land may impact the carbon cycle in the ocean due to the mobility of the water soluble labile fraction [11,12]. The knowledge of recalcitrance of carbon in biochar and the potential contamination from labile components are crucial issues for evaluating the agroenvironmental impact of biochar.

A number of approaches have been proposed to assess stability and the carbon sequestering potential of different biochars, including solid state nuclear magnetic resonance spectroscopy (solid state ^{13}C NMR) [13,14], thermal analysis (thermogravimetry, TG) [15,16], molecular markers by means of pyrolysis-gas chromatography-mass spectrometry (Py-GC-MS) [17,18], benzene polycarboxylic acid method [19], O:C or H:C molar ratios [20,21], chemical oxidation [14,22], accelerated ageing technique [23], and hydropyrolysis (HyPy) [24,25,26].

Among these techniques, the HyPy is interesting for the very high conversions of labile organic matter and accurate quantification of black carbon (BC) in different environmental matrices, including biochar [27] and biochar amended soil [8]. Moreover, HyPy integrated with GC-MS also allows for the molecular characterisation of the biochar semi-labile fraction defined as non-BC_{HyPy}. Additional benefits from HyPy include minimal product rearrangements and absence of generation of secondary char [28] as is often encountered in other chemical or thermal oxidative methods. In HyPy, the sample mixed with a sulphided molybdenum catalyst is pyrolyzed in the presence of hydrogen at high pressure to promote the reductive removal of thermally labile organic matter leaving a refractory and highly aromatic carbonaceous residue. This carbonaceous residue that remains after HyPy comprehends polyaromatic units greater than 7 fused rings [29,30] and can be quantified by elemental analysis. Therefore, HyPy method removes all labile organic matter (non-BC_{HyPy}), so isolating a highly stable portion of the biochar composed of highly condensed aromatic clusters and defined as BC_{HyPy} [25] or as stable polycyclic aromatic carbon (SPAC) [27,31]. The non-BC_{HyPy} fraction of chars that is evolved by thermal reductive cleavage has been shown to contain PAHs comprising ≤ 7 rings. Thus this fraction that is composed of ≤ 7 rings is supposed to be less permanent compared to larger PAH structures that constitute the BC_{HyPy} macromolecular network and has been defined as ``semi-labile'' [8]. This semi-labile fraction, due to its susceptibility to biological and chemical oxidation [27], is likely to be stable on timescales of years to decades. The labile fraction, which evolves on timescales of months to years, is also very important because can influence the soil microbial community structure [9,32]. HyPy was recently applied to investigate the impact of biochar amendment in an agricultural soil on the BC_{HyPy} and non-BC_{HyPy} fractions and their fate over time [8]. Biochar addition increased remarkably the BC_{HyPy} fraction, while the level of non-BC_{HyPy} PAHs was less influenced due to the large reservoir of these PAHs in original soil. However, more studies are needed to understand the role of this fraction in soil amended with biochar.

The aim of the present study is to quantify the BC_{HyPy} and characterise non-BC_{HyPy} fractions in biochar samples produced from different feedstock and process conditions with the same pyrolysis unit. Results were also compared with Py-GC-MS data to evaluate if these two analytical pyrolysis techniques provide a set of coherent complementary information on biochar stability and the molecular characteristics of thermally labile fraction. In particular, the attention was focused to the distribution of PAHs produced by HyPy and Py-GC-MS as molecular proxies.

<H1>2. Experimental

<H2>2.1. Samples

Three different types of biomass were used as feedstock materials: pine wood chips – with an average size of 3 cm × 2 cm × 0.5 cm – from Robeta Holz OHG, Milmersdorf, Germany; beech wood spheres – with a diameter of 25 mm, provided by Meyer and Weigand Gmbh, Nordlingen, Germany; corn digestate derived from maize silage.

Biochar samples were produced by pyrolysis of sample using a stainless steel fixed-bed reactor of 102.5 cm height and 22 cm of internal diameter. The inert atmosphere is provided by a N_2 flow entering the reactor (20 L min^{-1} and 50 L min^{-1}) from the bottom through a stainless steel grate to get a uniformly distributed flow. The samples (in the range of kilograms) were uniformly placed inside the reactor in a stainless steel container of 21 cm of diameter and 56 cm height which is placed directly on the previously mentioned grate. The reactor is externally heated with a wire heater with a maximum power of 3000 W placed on the external reactor wall. Both flanges in the reactor are also heated and insulated to reduce heat losses. The N_2 flow is preheated before entering the reactor as well. The temperature operation of this preheater is 600 °C.

Pyrolysis were performed at three different temperatures, 340 °C, 400 °C and 600 °C. The biochar samples obtained were labeled as PW400, PW600, BW340, BW600, CD400 and CD600 (where PW, BW, CD stand for pine wood, beech wood and corn digestate, respectively; 340, 400 and 600 indicated the pyrolysis temperatures in degrees centigrade) (Table 1).

<H2>2.2. Biochar bulk characterization

Biochar samples were thoroughly homogenized and oven-dried at 40 °C for 72 h, and stored at -20 °C prior to analysis. Elemental composition (CHNS) was determined by combustion using a Thermo Scientific FLASH 2000 Series CHNS/O Elemental Analyzer (Thermo Fisher Scientific, Waltham, U.S.A.). The biochar samples were acid tested for the presence of carbonates. The carbonate content of each biochar was determined on duplicate samples by comparing total organic carbon measured after hydrochloric acid (HCl) treatment and total carbon. In particular, about 3-4 mg of biochar sample were reacted with 40 µL of 1.5 M HCl and then heated at 60 °C for 1 hour; this procedure was repeated for 4-5 times, till the samples stop reacting with HCl. Only corn digestate biochars (CD600 5.1% and CD400 4.2%) were found to contain carbonates. The measured carbonate content values were used to correct the respective total carbon (TC) to total organic carbon (TOC) of biochar.

Ash was determined as the residual mass left after exposure at 600 °C for 5 hours. The oxygen content was calculated from the mass balance: Oxygen (%) = 100 - Ash content (%) - C (%) – H (%) - N (%). Moisture contents were determined (ASTM D-3173) at 105 °C.

<H2>2.3. Extractable polycyclic aromatic hydrocarbons (PAHs)

Analyses of extractable PAHs in biochars were conducted in triplicate as described in Fabbri et al. [33], but using 16 PAHs deuterated of each of the 16 US EPA PAHs instead of 3 PAHs deuterated. The measured PAHs included naphthalene, acenaphthylene, acenaphthene, fluorene, phenanthrene, anthracene, fluoranthene, pyrene, benzo(*a*)anthracene, chrysene, benzo(*b*)fluoranthene, benzo(*k*)fluoranthene, benzo(*a*)pyrene, dibenz(*ah*)anthracene, benzo(*ghi*)perylene, and indeno(1,2,3-*cd*)pyrene.

Briefly, about 0.5 g of biochar was spiked with 0.1 mL of a 5 mg L^{-1} solution of deuterated 16 EPA PAHs (prepared from Dr. Ehrenstorfer PAH-Mix 9 deuterated, 10 ng μL^{-1}) and soxhlet extracted with acetone/cyclohexane (1:1, v/v) for 36 hours. The solution was filtered, added with 1 ml of *n*-nonane (keeper to prevent the extraction solution being reduced to dryness with loss of analytes), carefully evaporated by rotatory vacuum evaporation at 40 °C and cleaned up by solid phase extraction onto a silica gel cartridge before analysis with a Agilent HP 6850 GC coupled to a Agilent HP 5975 quadrupole mass spectrometer (Agilent Technologies, Inc., Santa Clara, CA, U.S.A.); GC-MS conditions were those detailed in Fabbri et al. [33]. Recovery of deuterated PAHs was determined with respect to the internal standard 1,3,5-tri-*tert*-butylbenzene (10 mg L^{-1} Sigma-Aldrich). Results are reported as averages of three replicates analyses.

<H2>2.4. Analytical pyrolysis

<H3>2.4.1. Pyrolysis-GC/MS

Py-GC-MS analyses were performed using an electrically heated platinum filament CDS 5250 pyroprobe interfaced to a Varian 3400 GC equipped with a GC column (HP-5-MS; Agilent Technologies 30 m × 0.25 mm, 0.25 μm) and a mass spectrometer (Saturn 2000 ion trap, Varian Instruments) set at an electron ionization at 70 eV in full scan acquisition (10–450 *m/z*). A quartz sample tube containing of weighed biochar sample (5-10 mg) added with 1 μL of internal standard solution (*o*-isoeugenol at 1000 mg L^{-1} in methanol) was inserted into the Py-GC interface (300 °C) and then pyrolysed at 900 °C (set temperature) for 100 s with helium as carrier gas (100 mL min^{-1}). The following thermal program was used: 35 °C to 310 °C at 5 °C min^{-1}. On each biochar sample were performed two analysis and the pyrolysis products were quantified in terms of yields (μg g^{-1}) and relative abundance (%). Yields were

estimated from the ratio of the peak area integrated in the mass chromatogram of a characteristic ion of the selected pyrolysis product and the peak area of the internal standard, the quantity of added internal standard and the amount of sample pyrolysed [34], assuming an unitary relative response factor for each compound. In particular, a set of 33 pyrolysis products among the most abundant and representative of biological precursors was selected on the basis of a previous work [35] and total yields were the summed yields of these selected pyrolysis products (Table 3). Likewise a previous study [35], these pyrolysis products were grouped into three thermolabile class fractions: highly carbonised (charred), weakly carbonised hemi/cellulose and lignin (Table 3).

<H3>2.4.2. Hydropyrolysis

Hydropyrolysis (HyPy) tests were performed using the procedure described in detail elsewhere [8,25]. Briefly, 50-100 mg of biochar sample were loaded with a Mo catalyst using an aqueous/methanol 0.2 M solution of ammonium dioxydithiomolybdate [$(NH_4)_2MoO_2S_2$]. Catalyst weight was ~ 10% of the sample weight. The catalyst loaded biochar samples were placed within shortened borosilicate pipette ends (20 mm long), plugged at each end with pre-cleaned quartz wool and then placed in the HyPy reactor. We used the recommended temperature program previously optimized for pyrogenic carbon quantification where the samples are heated at rate of 300 °C min^{-1} from 50 to 250 °C, then heated at 8 °C min^{-1} from 250 °C until the final temperature of 550 °C for 2 min [24,25], all under a hydrogen pressure of 15 MPa. A controlled constant hydrogen sweep gas flow of 5 L min^{-1}, measured at ambient temperature and pressure, through the reactor bed ensured that the products (non-BC_{HyPy}) were quickly removed from the reactor, and subsequently trapped in a silica gel-filled trap cooled by dry ice [36].

Stable fraction (BC_{HyPy}). The BC_{HyPy} content of each biochar sample was derived by comparing the organic carbon (OC) content of the catalyst loaded samples prior to HyPy with those of their HyPy residues (Eq. (1)). The OC content was determined, after the decarbonation of the biochar sample, by combustion as described above.

$$BC_{HyPy}\,(BC/OC\ \%) = \frac{\text{weight of HyPy residue including spent catalyst}\,(\text{mg}) \times \text{OC}\,(\%)}{\text{initial weight of biochar including catalyst}\,(\text{mg}) \times \text{OC}\,(\%)}\ \text{x100} \quad (1)$$

Semi-labile fraction (non-BC_{HyPy}). The biochar non-BC_{HyPy} fractions were desorbed from the trap silica with 10 mL aliquots of *n*-hexane/dichloromethane (1:1, v/v). The eluents were

evaporated to dryness at room temperature for 12 h and the residues dissolved in 1 mL of dichloromethane prior to analysis. GC–MS analyses of the organic solutions concentrated, added with 100 µL internal standard solutions (*n*-hexatriacontane and 1,3,5-tri-*tert*-butylbenzene, 100 mg L^{-1} each), were performed on 6850 Agilent HP gas chromatograph connected to a 5975 Agilent HP quadrupole mass spectrometer (EI mode, 70 eV), equipped with an autosampler and a split/splitless injector. Analytes were separated by a HP-5MS fused silica capillary column (stationary phase poly[5% diphenyl/95% dimethyl]siloxane, 30 m × 0.25 mm i.d., 0.25 mm film thickness), using helium as the carrier gas, and an oven programme of 50 °C (hold for 2 min) to 300 °C (hold for 33 min) at 5 °C min^{-1}. Samples (1 µL) were injected under splitless conditions (1 min, then split ratio 1:50 to the end of analysis) with an injector temperature of 280 °C. Quantification of PAHs, alkylated PAHs and biphenyl was performed in full scan mode (*m/z* 35-650), using the mass chromatograms of the molecular ion of each compound and by comparison with added 1,3,5-tri-*tert*-butylbenzene using the relative response factors determined by single point calibration (PAH-Calibration Mix Supelco at 10 mg L^{-1} for each PAH. The 16 US EPA PAHs were identified by matching the retention times of each peak in the sample chromatogram with those of a standard solution. The identification of alkylated PAHs was based on comparisons with NIST mass spectra library (NIST MS Search r. 2.0). The concentration of individual *n*-alkanes was determined from *m/z* 57 mass chromatograms and by comparison with the added internal standard *n*-hexatriacontane assuming equal response factors for each compound. Procedural blank analyses showed absence of contamination.

<H2>2.5. Statistical analysis

Quantitative data are presented as mean values ± standard deviation (s.d., reported for triplicate and duplicate analyses as indicated by ``n"). In analyses of extractable PAHs the recovery of deuterated PAHs was (mean ± %RSD for all the data set, n = 3): 80% ± 6% naphthalene-d_8, 69% ± 27% acenaphthylene-d_8, 91% ± 4% acenaphthene-d_{10}, 88% ± 21% fluorene-d_{10}, 90% ± 17% phenanthrene-d_{10}, 70% ± 23% anthracene-d_{10}, 88% ± 10% fluoranthene-d_{10}, 87% ± 9% pyrene-d_{10}, 83% ± 18% chrysene-d_{12}, 84% ± 10% benzo(*a*)anthracene-d_{12}, 87% ± 11% benzo(*b*)fluoranthene-d_{12}, 79% ± 15% benzo(*k*)fluoranthene-d_{12}, 79% ± 23% benzo(*a*)pyrene-d_{12}, 75% ± 22% indeno(1,2,3-*c*,*d*)pyrene-d_{12}, 82% ± 12% dibenz(*ah*)anthracene-d_{14} and 77% ± 19% benzo(*ghi*)perylene-d_{12}. The RSD of the *o*-isoeugenol peak area was in the 5-26% interval. Student t tests were conducted with Excel (2011) to evaluate significant difference between two parameters of

biochar. Linear (Pearson) correlation coefficient between two variables r(df), where df stands for degrees of freedom, was determined for all the investigated parameters.

<H1>3. Results and discussion

<H2>3.1 Biochar characterization

Results of biochar characterizations are reported in Table 1. Pyrolysis temperature showed significant effect on elemental compositions of wood biochars and to a lesser extent on that of corn digestate biochars. In particular, carbon content of wood biochar increased with temperature, while the oxygen and hydrogen contents decreased. This resulted in lower H/C and O/C atomic ratio values at increasing final temperature (Table 1).

The degree of carbonisation of chars is generally expressed by molar H/C [14,21] or O/C ratios [19,20]. The O/C ratios of the investigated biochars ranged from 0.04 (PW600) to 0.24 (PW400) in accordance to the loss of oxygenated functionalities with increasing carbonisation [37], and were strongly correlated with molar H/C ratios (R = +0.96). The carbon and oxygen contents of beech and pine wood biochar were higher compared to that of corn digestate biochar, while this latter showed higher ash and nitrogen contents. The differences in ash and carbon contents can be linked to the chemical composition differences between wood and corn digestate. Wood contains more cellulose and hemicelluloses than digestate and during high temperature pyrolysis (> 500 °C); the components are reduced to carbon thus the higher carbon content in wood biochar [38,39].

The ash content of biochar samples was influenced mainly by feedstock and to a lesser extent by pyrolysis temperature with ash content increasing with pyrolysis temperature. The increase in ash content should result from progressive concentration of minerals and destructive volatilization of lignocelluloses matters as temperature increased [40]. However, the ash content of corn digestate biochar was much higher (up to 47.3%) than that in beech and pine wood biochar (up to 1.51%).

The concentrations of extractable PAHs ranged between 2.2 (BW340) and 18.9 μg g^{-1} (PW400) (Table SM2 in Supplementary Materials). However, it is interesting to note that despite the difference in feedstock at 600 °C the PAH levels were quite similar (2.2-2.9 μg g^{-1}), but significantly different at low temperature (340-400 °C). Therefore, the influence of feedstock type on PAHs concentration is evidenced by results obtained from biochar produced at low temperature. For beech wood and corn digestate biochar, naphthalene was the most abundant PAH, in accordance to previous studies [33,41,42], followed by

phenanthrene. While for the pine wood biochar the most abundant PAH was phenanthrene, followed by naphthalene in BW600 and by fluoranthene and pyrene in BW340.

<H2>3.2. BC_{HyPy} fraction

Figure 1 shows the concentrations of the BC_{HyPy} fraction in the different biochar samples (values reported in Table SM1 along with weight loss). The feedstock source and pyrolysis temperature clearly influenced the proportion of BC_{HyPy} and the degree of condensation of aromatic C. The wood biochars produced at 340-400 °C contained the lowest proportions of BC_{HyPy} fraction, with the pine wood biochar having lower proportions (15.7 ± 0.54%) than the biochar produced from beech wood (20.5 ± 5.0%). The relatively low BC_{HyPy} contents of the BW340 and PW400 biochars are to be expected due to the lower temperature of formation [18].

The BC_{HyPy} fraction in wood biochars obtained by pyrolysis at 600 °C was 89.7 ± 1.7% and 95.9 ± 0.7% beech and pine wood, respectively. These values were much higher than those found at 340-400 °C, demonstrating that pyrolysis temperature exerts a strong control on the formation of BC_{HyPy}. These results are consistent with those reported by Wurster et al. [26] and McBeath et al. [27], who showed that BC_{HyPy} content is largely controlled by the temperature of formation of biochar. The BC_{HyPy} content was <50% for biochars produced at temperatures ≤ 400 °C, 50-80% for biochars produced at 550°C, and >80% for biochars produced at temperatures ≥700 °C. We can presume that a dominant non-BC_{HyPy} fraction was formed at 340-400 °C by unimolecular cyclization, dehydrogenation, dealkylation, and aromatization reactions of wood constituents (lignin, hemicellulose, and cellulose as well as lipids such as resins) [43]. At 600 °C this fraction was condensed by pyrosynthesis into larger aromatic structures increasing the BC_{HyPy} [13,23,44]. The highly polycondensed aromatic moieties of BC_{HyPy} cannot be cracked into volatile compounds analyzable by GC-MS.

A different behaviour was observed in biochar from corn digestate that highlighted the importance of feedstock type on the degree of carbonisation. Corn digestate produced a thoroughly carbonised biochar (BC_{HyPy} 91%) even at 400 °C. This was reflected in (i) a low mass losses during HyPy; (ii) a high value of BC_{HyPy}; (iii) a low value of non-BC_{HyPy} fraction produced. The high content of BC_{HyPy} in CD400 could be explained by peculiar characteristics of the feedstock associated to the anaerobic digestion of corn silage that determines an increase of the biologically recalcitrant lignin fraction and ash. As reported by Kaal et al. [45], the lignin markers show a maximum at 280-300 °C and decrease with the increase of temperature until negligible contributions for pyrolysis temperatures > 400 °C.

Probably the high levels of lignin and ash in corn digestate favoured in comparison to wood favoured de-alkylation with formation of parent PAHs (see section 3.3) and condensation into large aromatic structures at lower temperatures.

The BC_{HyPy} content was inversely correlated with H/C (R = -0.99). The H/C ratio is indicative of the aromaticity degree [46] and carbonisation intensity [14,21] in turn associated with the stability of biochar [18,47]. Therefore BC_{HyPy} could be a parameter to be considered in order to characterise environmental recalcitrance of biochar and its sequestering potential.

<H2>3.3. non-BC_{HyPy} fraction

Figure 2 shows the total ion chromatograms of the non-BC_{HyPy} fraction derived from biochars. The PAHs detected and quantified (Table 2) in the biochars ranged from 2-ring compounds (naphthalene) to 7-ring compounds (coronene). This range of ring size is similar to that generated by HyPy from charcoals [29,48], and the definition of BC_{HyPy} as being composed of PAHs with >7 rings proposed by Meredith et al. [25]. The non-BC_{HyPy} fraction composed of <7 aromatic rings known to be biodegradable [49] and susceptible to biological and chemical oxidation [27]. The non-BC_{HyPy} fraction was found to be an important reservoir of PAHs in soil [8]. The non-stable fraction (non-BC_{HyPy} and labile fraction), which evolves from biochar during its storage in soil, is likely to impact on microbial activity [9,32], and therefore affects the functioning of the soil as a whole, including the balance of indigenous labile pools [10,50]. However, the properties of biochar non-stable fraction derived from various biomasses are different [14], and thus their effects on soil should be different. The labile fraction can have positive effects on soil microorganisms, increasing microbial biomass [32,51], with increase in CO_2 emission from the decomposition of native soil organic carbon [22,52], or in some case negative effects on soil microorganisms with decrease [53] in CO_2 emission. In fact, the microorganisms can utilize a number of labile biochar constituents as an energy source [22]. While some biochar associated labile components have biocidal activity [54], which may increase its stability against biotic decomposition. For instance, previous studies have shown that the inhibitory component of deleterious some biochars is likely to be low molecular weight organic acids and phenols [55,56].

Interestingly, partially hydrogenated PAHs were observed in non-BC_{HyPy} fractions of almost all biochars. In particular, partially hydrogenated fluoranthene, pyrene small amounts of phenanthrene were tentatively identified in the MS-hydropyrolysates of BW340, BW600, PW400, PW600 and CD400 biochars. Only HyPy treatment of CD600 did not release detectable levels of partially hydrogenated PAHs probably due to the low levels of PAHs. As

reported in a previous study [57], the hydrogenation of aromatic compounds is an artefact of the HyPy method, probably influenced by the characteristics of the matrix. Small amounts of partially hydrogenated PAHs were recently observed from the HyPy of soil treated biochar at levels higher than those of original biochar [8]. Moreover, considering the abundance of parent PAHs, the results suggest that the hydrogenation of PAH is closely linked to stability as the major presence of pericondensed PAHs (e.g. pyrene) with respect to catacondensed PAHs (e.g. phenanthrene). This is in accordance with Grotheer et al. [57], who found PAHs vulnerability to hydrogenation in HyPy treatment and that this reaction was controlled by the relative structural stability of the PAHs.

Almost all PAHs could be quantified in the biochars produced at lower temperatures, while in all of the biochars at 600 °C PAHs occurred at lower levels (Table 2). Concentrations of priority PAHs ranged from 43 µg g^{-1} to 6900 µg g^{-1}, with the lower values found for corn digestate probably because of the higher ash amount. For the same biomass, the concentrations were lower for biochar samples produced at higher temperatures. Semi-labile PAHs were found in an agricultural soil at levels around 20 µg g^{-1} [8] probably due to the presence black carbon normally present in the environment [58]. In the case of biochars from wood, the levels of non-BC_{HyPy} PAHs were much larger suggesting that their application in soil can contribute significantly to this fraction of organic carbon. PAHs can pose a short or long-term threat to soil and the environment by influencing the soil microbial activity [32], increasing in some case the persistence of mobile PAHs [59]. Therefore, the evaluation of the non-BC_{HyPy} fraction as a potential source of mobile PAHs is an important environmental aspect. Although, the concentrations of bioavailable PAHs seem to be very low [60].

A detailed analysis of the contribution of the individual PAHs in biochars produced at 600 °C indicated the dominance of 3-4 ring PAHs, phenanthrene (8-38% of the total PAHs), fluoranthene (15-28% of the total PAHs) and pyrene (36-61% of the total PAHs). While in the wood biochars at lower temperatures the PAHs with 5-7 rings composed almost the majority of PAHs. In fact, the 3-4 ring PAH /total (3-7 ring) PAH ratio was about 0.5 for BW340 and PW400, and about 1 for PW600 and CD600 (Table 2). Therefore, it can be assumed that biochar generated at a temperature of 340-400 °C will have an aromatic structure that is not sufficiently condensed to include ring cluster size greater than 7 (coronene) [24-26]. However, also in the biochar CD400, phenanthrene, fluoranthene and pyrene dominated the PAH profiles, supplying 28%, 14% and 45% of the total PAH concentrations, respectively. This ring size distribution of CD400, similar to that reported for biochars produced at 600 °C,

and the lower values of PAHs concentration in comparison to wood-derived biochars could be explained by the different composition of corn digestate characterized by a high content of ash and undigested biopolymers (lignin).

The non-BC_{HyPy} fraction of wood biochar at lower temperature comprised also alkylated PAHs. In particular, the following alkylated PAHs were detected in non-BC_{HyPy} fractions: C_1- to C_4-naphthalenes, C_1- to C_3-fluorenes, C_1- to C_3 phenanthrenes, C_1- to C_2-pyrenes, C_1- to C_2-chrysenes. For quantitative analyses, only methylated PAHs were selected (Table 2). The amounts of these compounds decrease with increasing temperature in wood biochar from 3400 µg g^{-1} to 330 µg g^{-1} for beech wood and from 3300 µg g^{-1} to 75 µg g^{-1} for pine wood.

The non-BC_{HyPy} of biochar CD600 is dominated by *n*-alkanes in the range C18 to C35 (the low carbon number compounds having been lost to evaporation), with a distribution centered at C26 and C28 and two maxima at C18 and C26. Fatty acids are a more probable source of these alkanes. Long chain fatty acids (C20-C34) are common component of the epicuticular waxes of maize [61]. Moreover, the maize used in anaerobic digestion is in a stage of ripeness (end of wax ripeness) [62] with content of long-chain fatty acids esters in waxes of 50% [63]. Carboxylic acids are known to be hydrogenated under HyPy conditions to form the corresponding even-numbered *n*-alkanes [64,65]. The presence of an aliphatic component and the high level of ash made these biochar different from typical woody biochar. It cannot be excluded that the inorganic constituents may influence the results of HyPy (and Py-GC-MS as well) that might explain similar trends different from those observed for wood-derived biochars.

<H2>3.4. HyPy comparison with Py-GC-MS

The molecular signature of the thermally labile fraction of biochar was also examined by flash pyrolysis (Py-GC-MS), and its association with HyPy GC-MS investigated. The results of Py-GC-MS analysis, as for HyPy results, showed that the feedstock and pyrolysis temperature clearly influenced the molecular composition of thermally labile fraction (Table 3).

The pyrograms resulting from Py-GC-MS of biochar samples are depicted in Figure 3. The pyrolysates of all biochar samples were featured by the presence of aromatic hydrocarbons including benzene, benzene derivatives, and polycyclic aromatic hydrocarbons (PAHs; e.g., naphthalene, phenanthrene). The pyrolysis products lignin markers, represented by 2-methoxyphenols (guaiacols), 4-vinylguaiacol, 4-methylguaiacol, 4-ethylguaiacol, 4-methylsyringol and 2,5-dimethoxyphenols (syringols), were abundant in the pyrolysate of

PW400 and BW340 biochar, while these lignin markers were not detected in PW600, BW600, CD600. Interestingly, lignin markers were not observed in CD400; this is in accordance with the high content of BC_{HyPy}. The phenols and methylphenols, which are less specific lignin markers, were abundant in PW400 and BW340, but were detected also in corn digestate biochars. In this case, the phenols and methylphenols are therefore of little diagnostic value with respect to highly or weakly pyrolysed lignin. Phenols were not revealed in the non-BC_{HyPy} fractions; however, the analytical procedure was developed for the characterisation of hydrocarbons. Pyrograms rich in phenol derivatives suggest that thermally labile fraction is characterized by partially charred lignin. These of phenolic species, as described above, can be responsible of toxic effects on seedling growth [55]. Interestingly, phenols and other oxygenated were identified in the water extracts of biochar [66]. The importance of oxygenated structures in the semi-labile fraction of biochar requires further investigations.

The estimated total yields of pyrolysis products selected for quantitation varied over three orders of magnitude, spanning from 2.7 10^6 µg g^{-1} (PW400) down to 192 µg g^{-1} (PW600), with high yields for the biochar characterized by the highest temperature production (600 °C) and the highest content of ash (corn digestate biochar). Not surprisingly, the highest yields were obtained with low temperatures (340 and 400 °C) that presented the lowest levels of BC_{HyPy} (Figure 3). This firstly supports the view that Py-GC-MS provide additional information on the semi-labile fraction (non-BC_{HyPy}) of biochar. The proportion of charred products ranged from 37% (PW400, BW340) to >99% (PW600, BW600) (Table 3) in analogy with % BC_{HyPy} (Figure 1). Corn digestate biochars prepared at 400 and 600 °C presented both high levels of BC_{HyPy} and % charred Py-GC-MS.

The degree of alkylation is a molecular index of biochar thermal stability as proposed by Calvelo Pereira et al. [14] and confirmed by several studies [18,35,45]. The methyl/parent PAH ratios of selected PAHs, naphthalene from Py-GC-MS and phenathrene and pyrene from HyPy are presented in Table 4. In the case of biochars from wood, the ratios were lower for the most charred biochars prepared at 600 °C in accordance to dealkylation processes occurring at high temperatures. In particular, as reported in previous study [1], the values of alkylated compound decline sharply at pyrolysis temperature >400 °C. In fact, with increasing pyrolysis temperature from 340-400 °C to 600 °C, the Py-GC-MS and non-BC_{HyPy} alkylated PAHs are largely de-alkylated with formation of parent PAHs.

The non-BC_{HyPy} parent and alkylated PAHs are probably covalently bond or strongly sorbed onto aromatic surfaces, nanopores, or occluded sites of the BC_{HyPy} matrix [58] and therefore these aromatics compounds can be protected by the macromolecular structure against the destruction by thermal stress and weathering. However, the degree of de-alkylation of molecules detected by HyPy GC-MS, as showed by methyl/parent PAH ratios (Table 4), is very similar to those of free aromatic hydrocarbons obtained by Py-GC-MS.

<H1>4. Conclusions

This study is the first comprehensive and quantitative study of the semi-labile (non-BC_{HyPy}) fraction released from biochars generated from different feedstocks over a range of temperatures, and also includes a comparison of the non-BC_{HyPy} fraction produced to that from the Py-GC-MS of the same suite of biochars.

HyPy provided consistent information concerning the thermal stability of biochar samples, with the BC_{HyPy} contents showing a very strong inverse correlation with the molar H/C composition of the biochars (R = -0.99).

The non-BC_{HyPy} fractions were composed of a range of PAHs from two to seven rings, including alkylated derivatives up to C4, together with partially hydrogenated PAHs. The yields of PAHs in the non-BC_{HyPy} fraction were higher for those biochars produced at lower temperatures for all three feedstocks, and always greatly more abundant than the levels of solvent-extractable PAHs. The quantitative results indicated that contribution of non-BC_{HyPy} given by the application of biochar in soil could be significant and worth of investigation.

Comparing HyPy and Py-GC-MS data similar trends were observed for the % BC_{HyPy} and % charred (Py-GC-MS) values. HyPy and Py-GC-MS concordantly showed lower methylated/parent PAH ratios for the most charred biochars. However, the ring size distribution of Py-GC-MS products was not similar to that generated by HyPy. The non-BC_{HyPy} fraction was dominated by PAHs with >3 rings, while Py-GC-MS released mainly PAHs with < 3 rings along with monocyclic aromatic hydrocarbons. Moreover, Py-GC-MS showed the presence of oxygenated compounds, mostly phenols, in the less carbonised biochars suggesting that non-hydrocarbon structures could be present in the non-BC_{HyPy} fraction that were not revealed with the adopted analytical procedures. Furthermore, partially hydrogenated PAHs (e.g. dihydropyrene) were also observed in the non-BC_{HyPy}, suggesting PAHs vulnerability to hydrogenation in HyPy treatment.

<ACK>**Acknowledgements**

A.G.R. thanks the Department of Chemistry ``Giacomo Ciamician" *Alma Mater Studiorum* Università di Bologna for the grant Marco Polo to the National Environmental Research

Council (NERC standard grant number, NE/F017456/1) for developing hydropyrolysis to characterize the thermally labile fraction of biochar at the University of Nottingham. D.F. thanks the Italian Ministero dell'Istruzione, dell'Università e della Ricerca and the *Alma Mater Studiorum* Università di Bologna for financial support.

<REF>References
<BIBL>
[1] J. Lehmann, S. Joseph,;1; Biochar for Environmental Management, Science, Technology and Implementation, Science And Technology, second ed., <PN>Routledge</PN>, <PL>London</PL>, 2015.
[2] N.P. Gurwick, L.A. Moore, C. Kelly, P. Elias,;1; A systematic review of biochar research, with a focus on its stability in situ and its promise as a climate mitigation strategy. PLoS ONE 8 (9) (2013) e75932.
[3] Y. Kuzyakov, I. Bogomolova, B. Glaser,;1; Biochar stability in soil: Decomposition during eight years and transformation as assessed by compound-specific ^{14}C analysis, Soil Biol. Biochem. 70 (2014) 229−236.
[4] M. Zimmermann, M.I. Bird, C. Wurster, G. Saiz, I. Goodrick, J. Barta, P. Capek, H. Santruckova, R. Smernik,;1; Rapid degradation of pyrogenic carbon, Glob. Change. Biol. 18 (2012) 3306−3316.
[5] Y. Fang, B. Singh, B.P. Singh, E. Krull,;1; Biochar carbon stability in four contrasting soils, Eur. J. Soil Sci. 65 (2014) 60–71.
[6] T. Xie; B. Sadasivam; S.M. Asce; K.R. Reddy, F. Asce; C. Wang; K. Spokas,;1; Review of the Effects of Biochar Amendment on Soil Properties and Carbon Sequestration, J. Hazard. Toxic Radioact. Waste 20 (1) (2016) 04015013.
[7] K.A. Spokas, J. M: Novak, C.A. Masiello, M.G. Johnson, E.C. Colosky, J.A. Ippolito, C. Trigo,;1; Physical disintegration of biochar: an overlooked process, Environ. Sci. Tech. Lett. 1 (2014) 326–332.
[8] A.G. Rombolà, W. Meredith, C.E. Snape, S. Baronti, L. Genesio, F.P. Vaccari, F. Miglietta, D. Fabbri,;1; Fate of Soil Organic Carbon and Polycyclic Aromatic Hydrocarbons in a Vineyard Soil Treated with Biochar, Environ. Sci. Technol. 49 (2015) 11037–11044.
[9] J. Lehmann, M.C. Rillig, J. Thies, C.A. Masiello, W.C. Hockaday, D. Crowley,;1; Biochar effects on soil biota – a review, Soil Biol. Biochem. 43 (2011) 1812–1836.
[10] N. Ameloot, S. Sleutel, S.D.C. Case, G. Alberti, N.P. McNamara, C. Zavalloni, B. Vervisch, G. delle Vedove, S. De Nevea,;1; C mineralization and microbial activity in four biochar field experiments several years after incorporation, Soil Biol. Biochem. 78 (2014) 195–203.
[11] R. Jaffé, Y. Ding, J. Niggemann, A.V. Vähätalo, A. Stubbins, R.G.M. Spencer, J. Campbell, T. Dittmar,;1; Global charcoal mobilization from soils via dissolution and riverine transport to the oceans, Science 340 (2013) 345−347.
[12] J. Kaal, S. Wagner, R. Jaffé,;1; Molecular properties of ultrafiltered dissolved organic matter and dissolved black carbon in headwater streams as determined by pyrolysis-GC–MS, J. Anal. Appl. Pyrolysis (2016), <DOI>10.1016/j.jaap.2016.02.003, <C>in press</C></DOI>
[13] A. V. McBeath, R. J. Smernik,;1; Variation in the degree of aromatic condensation of chars, Org. Geochem. 40 (2009) 1161–1168.
[14] R. Calvelo Pereira, J. Kaal, M. Camps Arbestain, R. Pardo Lorenzo, W. Aitkenhead, M. Hedley, F. Macías, J. Hindmarsh, J.A. Maciá-Agulló,;1; Contribution to characterisation of biochar to estimate the labile fraction of carbon, Org. Geochem. 42 (2011) 1331–1342.

[15] J. M. de la Rosa, H. Knicker, E. López-Capel, D.A.C. Manning, J.A. González-Perez, F.J. González-Vila,;1; Direct detection of black carbon in soils by Py–GC/MS, ^{13}C NMR spectroscopy and thermogravimetric techniques, Soil Sci. Soc. Am. J. 72 (2008) 258–267.
[16] R. Zornoza, F. Moreno-Barriga, J.A. Acosta, M.A. Munoz, A. Faz,;1; Stability, nutrient availability and hydrophobicity of biochars derived from manure, crop residues, and municipal solid waste for their use as soil amendments, Chemosphere 144 (2016) 122–130.
[17] J. Kaal, C. Rumpel,;1; Can pyrolysis–GC/MS be used to estimate the degree of thermal alteration of black carbon? Org. Geochem. 40 (2009) 1179–1187.
[18] R. Conti, A.G. Rombolà, A. Modelli, C. Torri, D. Fabbri.;1; Evaluation of the thermal and environmental stability of switchgrass biochars by Py–GC–MS, J. Anal. Appl. Pyrolysis 110 (2014) 239–247.
[19] S. Brodowski, A. Rodionov, L. Haumaier, B. Glaser, W. Amelung,;1; Revised black carbon assessment using benzene polycarboxylic acids, Org. Geochem. 36 (2005) 1299–1310.
[20] K.A. Spokas,;1; Review of the stability of biochar in soils: predictability of O:C molar ratios, Carbon Manage. 1 (2010) 289–303.
[21] A. Enders, K. Hanley, T. Whitman, S. Joseph, J. Lehmann,;1; Characterization of biochars to evaluate recalcitrance and agronomic performance, Bioresour. Technol. 114 (2012) 644–653.
[22] A. Cross, S.P. Sohi,;1; A method for screening the relative long-term stability of biochar, GCB Bioenergy 5 (2013) 215–220.
[23] O. Mašek, P. Brownsort, A. Cross, S. Sohi,;1; Influence of production conditions on the yield and environmental stability of biochar, Fuel 103 (2013) 151–155.
[24] P.L. Ascough, M.I. Bird, F. Brock, T.F.G. Higham, W. Meredith, C.E. Snape, C.H. Vane,;1; Hydropyrolysis as a new tool for radiocarbon pre-treatment and the quantification of black carbon, Quat. Geochronol. 4 (2009) 140–147.
W. Meredith, P.L. Ascough, M.I. Bird, D.J. Large, C.E. Snape, Y. Sun, E.L. Tilston,;1; Assessment of hydropyrolysis as a method for the quantification of black carbon using standard reference materials, Geochim. Cosmochim. Acta 97(2012) 131–147.
[25] C.M. Wurster, G. Saiz, M.P.W. Schneider, M.W.I. Schmidt, M.I. Bird,;1; Quantifying pyrogenic carbon from thermosequences of wood and grass using hydrogen pyrolysis, Org. Geochem. 62 (2013) 28–32.
[26] A.V. McBeath, C.M. Wurster, M.I. Bird,;1; Influence of feedstock properties and pyrolysis conditions on biochar carbon stability as determined by hydrogen pyrolysis, Biomass Bioenergy 73 (2015) 155–173.
[27] G.D. Love, C.E. Snape, A.D. Carr, R.C. Houghton,;1; Release of covalently-bound alkane biomarkers in high yields from kerogen via catalytic hydropyrolysis, Org. Geochem. 23 (1995) 981–986.
[28] P.L. Ascough, M.I. Bird, W. Meredith, R.E. Wood, C.E. Snape, F. Brock, T.F.G. Higham, D. Large, D. Apperley,;1; Hydropyrolysis: Implications for radiocarbon pre-treatment and characterization of Black Carbon, Radiocarbon 52 (2010) 1336–1350.
[29] C.M. Wurster, J. Lloyd, I. Goodrick, G. Saiz, M.I. Bird,;1; Quantifying the abundance and stable isotope composition of pyrogenic carbon using hydrogen pyrolysis, Rapid Commun. Mass Spectrom. 26 (2012) 2690–2696.
[30] C.M. Wurster, A.V. McBeath, M.I. Bird,;1; The carbon isotope composition of semi-labile and stable pyrogenic carbon in a thermosequence of C_3 and C_4 derived char, Org. Geochem. 81 (2015), 20–26.
[31] N. Ameloot, E.R. Graber, F.G.A. Verheijen, S. De Neve,;1; Interactions between biochar stability and soil organisms: review and research needs, Eur. J. Soil Sci. 64 (2013) 379–390.

[32] D. Fabbri, A.G. Rombolà, C. Torri, K.A. Spokas,;1; Determination of polycyclic aromatic hydrocarbons in biochar and biochar amended soil, J. Anal. Appl. Pyrolysis 103 (2013) 60–67.
[33] C. Torri, A. Adamiano, D. Fabbri, C. Lindfors, A. Monti, A. Oasmaa,;1; Comparative analysis of pyrolysate from herbaceous and woody energy crops by Py–GC with atomic emission and mass spectrometric detection, J. Anal. Appl. Pyrolysis 88 (2010) 175–180.
[34] D. Fabbri, C. Torri, K.A. Spokas,;1; Analytical pyrolysis of synthetic chars derived from biomass with potential agronomic application (biochar). Relationships with impacts on microbial carbon dioxide production, J. Anal. Appl. Pyrolysis 93 (2012) 77–84.

[35] W. Meredith, C.A. Russell, M. Cooper, C.E. Snape, G.D. Love, D. Fabbri, C.H. Vane,;1; Trapping hydropyrolysates on silica and their subsequent thermal desorption to facilitate rapid fingerprinting by GC-MS, Org. Geochem. 35 (2004) 73–89.

[36] E.S. Krull, J. Baldock, J.O. Skjemstad, R.J. Smernik,;1; Characteristics of biochar:organo-chemical properties, in: J. Lehmann, S. Joseph (Eds.), Biochar for Environmental Management: Science and Technology, <PN>Earthscan</PN>, <PL>London</PL>, 2009, pp. 53–65.

[37] M. Keiluweit, S. Nico Pete, G. Johnson Mark, M. Kleber,;1; Dynamic molecular structure of plant biomass-derived black carbon (biochar), Environ. Sci. Technol. 44 (2010) 1247–1253.

[38] M.I. Al-Wabel, A. Al-Omran, A.H. El-Naggar, M. Nadeem, A.R. Usman,;1; Pyrolysis temperature induced changes in characteristics and chemical composition of biochar produced from conocarpus wastes, Bioresour. Technol. 131 (2013) 374–379.

[39] W.T. Tsai, S.C. Liu, H.R. Chen, Y.M. Chang, Y.L. Tsai,;1; Textural and chemical properties of swine-manure-derived biochar pertinent to its potential use as a soil amendment, Chemosphere 89 (2012) 198–203.

[40] S.E. Hale, J. Lehmann, D. Rutherford, A.R. Zimmerman, R.T. Bachmann, V.Shitumbanuma, A. O'Toole, K.L. Sundqvist, H. Hans Peter, H.P.H. Arp, G. Cornelis-sen,;1; Quantifying the total and bioavailable polycyclic aromatic hydrocarbonsand dioxins in biochars, Environ. Sci. Technol. 46 (2012) 2830–2838.

[41] I. Hilber, F. Blum, J. Leifeld, H.-P. Schmidt, T.D. Bucheli,;1; Quantitative determination of PAHs in biochar: a prerequisite to ensure its quality and safe application, J. Agric. Food Chem. 60 (2012) 3042–3050.

[42] X. Li, Q. Shen, D. Zhang, X. Mei, W. Ran, Y. Xu, G. Yu,;1; Functional groups determine biochar properties (pH and EC) as studied by two-dimensional 13C NMR correlation spectroscopy, PloS One 8 (2013) e65949.

[43] B.T. Nguyen, J. Lehmann, W.C. Hockaday, S. Joseph, C.A. Masiello,;1; Temperature sensitivity of black carbon decomposition and oxidation, Environ. Sci. Technol. 44 (2010) 3324–3331.

[44] J. Kaal, M.P.W. Schneider, M.W.I. Schmidt,;1; Rapid molecular screening of black carbon (biochar) thermosequences obtained from chestnut wood and rice straw: a pyrolysis–GC/MS study, Biomass Bioenergy 45 (2012) 115–129.

[45] T. Wang, M. Camps-Arbestain, M. Hedley,;1; Predicting C aromaticity of biochars based on their elemental composition, Org. Geochem. 62 (2013) 1–6.

[46] K. Crombie, M. Ondřej, S.P. Saran, B. Peter, C. Andrew,;1; The effect of pyrolysis conditions on biochar stability as determined by three methods, GCB Bioenergy 5 (2013) 122–131.

[47] X. Zhang, D. Huang, H. Deng, C. Snape, W. Meredith, Y. Zhao, Y. Du, X. Chen, Y. Sun,;1; Radiocarbon dating of charcoal from the Bianjiashan site in Hangzhou: New evidence for the lower age limit of the Liangzhu Culture, Quat. Geochronol. 30 (2015) 9–17.

[48] R. A. Kanaly, S. Harayama,;1; Biodegradation of high-molecular-weight polycyclic aromatic hydrocarbons by bacteria, J. Bacteriol. 182 (2000) 2059–2067.

[49] M.-A. de Graaff, A.T. Classen, H.F. Castro, C.W. Schadt,;1; Labile soil carbon inputs mediate the soil microbial community composition and plant residue decomposition rates. The New phytol. 188 (2010) 1055–1064.

[50] J.D. Gomez, K. Denef, C.E. Stewart, J. Zheng, M.F. Cotrufo,;1; Biochar addition rate influences soil microbial abundance and activity in temperate soils, Eur. J. Soil Sci. 65 (2014) 28–39.

[51] J.L. Smith, H.P. Collins, V.L. Bailey,;1; The effect of young biochar on soil respiration, Soil Biol. Biochem. 42 (2010) 2345–2347.

[52] W. Lu, W. Ding, J. Zhang, Y. Li, J. Luo, N. Bolan, Z. Xie,;1; Biochar suppressed the decomposition of organic carbon in a cultivated sandy loam soil: a negative priming effect, Soil Biol. Biochem. 76 (2014) 12–21.

[53] E.R. Graber, Y.M. Harel, M. Kolton, E. Cytryn, A. Silber, D.R. David, L. Tsechansky, M. Borenshtein, Y. Elad,;1; Biochar impact on development and productivity of pepper and tomato grown in fertigated soilless media, Plant Soil 337 (2010) 481–496.

[54] C.R. Smith, E.M. Buzan, J.W. Lee,;1; Potential impact of biochar water-extractable substances on environmental sustainability, ACS Sustain. Chem. Eng. 1 (2013) 118−126.

[55] W. Buss, O. Mašek, M. Graham, D. Wüst,;1; Inherent organic compounds in biochar – Their content, composition and potential toxic effects, J. Environ. Manage. 156 (2015) 150−157.

[56] H. Grotheer, A.M. Robert, P.F. Greenwood, K. Grice,;1; Stability and hydrogenation of polycyclic aromatic hydrocarbons during hydropyrolysis (HyPy) – relevance for high maturity organic matter, Org. Geochem. 86 (2015) 45–54.

[57] W. Meredith, P.L. Ascough, M.I. Bird, D.J. Large, C.E. Snape, J. Song, Y. Sun, E.L. Tilston,;1; Direct evidence from hydropyrolysis for the retention of long alkyl moieties in

black carbon fractions isolated by acidified dichromate oxidation, J. Anal. Appl. Pyrolysis 103 (2013) 232−239.

[58] R.S. Quilliam, S. Rangecroft, B.A. Emmett, T.H. Deluca, D.L. Jones,;1; Is biochar a source or sink for polycyclic aromatic hydrocarbon (PAH) compounds in agricultural soils? GCB Bioenergy 5 (2013) 96−103.

[59] P. Mayer, I. Hilber, V. Gouliarmou, S. E. Hale, G. Cornelissen, T. D. Bucheli,;1; How to Determine the Environmental Exposure of PAHs Originating from Biochar, Environ. Sci. Technol. 50 (2016) 1941−1948.

[60] R. Lessire, M. Hartmann-Bouillon, C. Cassagne,;1; Very long chain fatty acids: Occurrence and biosynthesis in membrane fractions from etiolated maize coleptiles, Phytochemistry 21 (1982) 55–59.

[61] R. Gao, Y. Xufeng, Z. Wanbin, W. Xiaofen, C. Shaojiang, C. Xu, Z. Cui,;1; Methane yield through anaerobic digestion for various maize varieties in China, Bioresour. Technol. 118 (2012) 611–614.

[62] P. Avato, G. Bianchi, N. Pogna,;1; Chemosystematics of surface lipids from maize and some related species, Phytochemistry 29 (1990) 1571–1576.

[63] M.A. Sephton, W. Meredith, C.-G. Sun, C.E. Snape,;1; Hydropyrolysis as a preparative method for the compound-specific carbon isotope analysis of fatty acids, Rapid Commun. Mass Spectrom. 19 (2005) 323–325.

[64] W. Meredith, C.-G. Sun, C.E. Snape, M.A. Sephton, G.D. Love,;1; The use of model compounds to investigate the release of covalently bound biomarkers via hydropyrolysis, Org. Geochem. 37 (2006) 1705–1714.

[65] A.G. Rombolà, G. Marisi, C. Torri, D. Fabbri, A. Buscaroli, M. Ghidotti, A. Hornung,;1; Relationships between Chemical Characteristics and Phytotoxicity of Biochar from Poultry Litter Pyrolysis, J. Agric. Food Chem. 63 (2015b) 6660–6667.

</BIBL>

<Figure>**Figure 1.** BC_{HyPy} (% OC) of biochar samples.

<Figure>**Figure 2.** Total ion chromatograms of the non-BC_{HyPy} fraction from HyPy of biochar samples (BW340, BW600, PW400, PW600, CD400 and CD600). C*x*, *n*-alkanes with *x* carbon atoms; ∗, probably hydrogenated PAHs. Internal standard: is, 1,3,5-tri-*tert*-butylbenzene; is*, *n*-hexatriacontane.

<Figure>**Figure 3.** Total ion chromatograms from Py-GC-MS of biochar BW340, BW600, PW400, PW600, CD400 and CD600. Internal standard: (is) *o*-isoeugenol.

Tables and figures

<Table>Table 1**.** Biomass feedstock, pyrolysis conditions, elemental molar ratios, elemental analysis, ash and moisture (mean values ± s.d., n = 3) of biochars samples (#: Sample identifiers).

Raw material	Volatiles (%)	Max T (°C)	N_2 flow L min^{-1}	H/C (molar)	O/C (molar)	C (%)	H (%)	N (%)	O (%)	Ash (%)	
Beech wood	-	340	50	0.72	0.23	71.9 ± 2.4	4.33 ± 0.092	0.18 ± 0.005	22.4 ± 2.4	1.14 ± 0.08	0
Beech wood	9.93	600	20	0.29	0.08	87.6 ± 2.8	2.14 ± 0.18	0.19 ± 0.047	9.3 ± 2.0	1.51 ± 0.04	0
Pine wood	33.70	400	20	0.70	0.24	71.7 ± 0.81	4.20 ± 0.064	0.18 ± 0.011	22.9 ± 0.89	1.06 ± 0.02	0
Pine wood	10.30	600	20	0.33	0.04	91.6 ± 2.3	2.50 ± 0.069	0.21 ± 0.017	4.4 ± 2.4	1.32 ± 0.04	0
Corn igestate	15.93	400	20	0.33	0.07	43.8 ± 0.51	1.21 ± 0.074	1.91 ± 0.048	3.80 ± 1.0	45.07 ± 0.05	0
Corn igestate	12.66	600	20	0.25	0.07	41.3 ± 0.36	0.86 ± 0.019	1.58 ± 0.004	3.87 ± 0.43	47.27 ± 0.04	0

<Table>Table 2**.** Estimated yields of PAHs and methylated PAHs (MePAHs) released by HyPy (non-BC_{HyPy} fraction) of biochar samples. Mean values ± s.d. (n = 2).

	BW340	BW600	PW400	PW600	CD400	CD600
	μg $g_{biochar}^{-1}$					
ene	8.0 ± 3.8	n.d.	57 ± 30	n.d.	n.d.	n.d.
halenes (2 isomers)	39 ± 12	n.d.	109 ± 11	n.d.	n.d.	n.d.
	28.0 ± 0.5	n.d.	96 ± 24	n.d.	n.d.	n.d.
hene	47.5 ± 2.2	n.d.	77 ± 11	n.d.	n.d.	n.d.
	161 ± 33	14.4 ± 0.2	416 ± 45	3.70 ± 0.7	14.2 ± 0.9	n.d.
enes (2 isomers)	255 ± 46	40 ± 4.5	446 ± 1.5	n.d.	23.0 ± 5.9	n.d.
rene	335 ± 80	579 ± 9.2	1019 ± 32	186 ± 41	257 ± 46	3.41 ± 0.0
nthrenes (2 isomers)	322 ± 46	92.8 ± 5.5	644 ± 2.5	27.9 ± 3.4	56 ± 13	n.d.
ne	74 ± 14	18.4 ± 0.3	166 ± 9	20.5 ± 0.7	13.4 ± 2.1	1.33 ± 0.0
acenes (2 isomers)	159 ± 35	16.9 ± 0.4	303 ± 21	n.d.	20 ± 5.3	n.d.
ene	289 ± 61	225 ± 7.1	548 ± 27	111 ± 7.3	126 ± 5.2	11.9 ± 2.8
nthenes (2 isomers)	322 ± 52	46.2 ± 4.9	558 ± 1.0	11.9 ± 0.6	41 ± 12	n.d.
	432 ± 102	540 ± 14	938 ± 14	239 ± 49	406 ± 71	26.0 ± 6.3
e (2 isomers)	464 ± 84	110 ± 14	691 ± 29	35.3 ± 6.3	81 ± 9.3	n.d.
	186 ± 45	53.2 ± 3.5	265 ± 24	19.8 ± 1.4	5.8 ± 0.7	n.d.
rysene	158 ± 28	2.72 ± 0.03	266 ± 1.0	n.d.	3.8 ± 0.8	n.d.
anthracene	150 ± 26	19.0 ± 0.4	346 ± 13	10.7 ± 1.3	18.3 ± 3.3	n.d.
nzo[a]anthracene	234 ± 22	14.0 ± 0.2	311 ± 6	n.d.	10.0 ± 1.5	n.d.
fluoranthene	384 ± 60	32.9 ± 0.9	734 ± 30	n.d.	21.5 ± 1.0	n.d.
fluoranthene	266 ± 59	24.4 ± 1.7	470 ± 18	n.d.	17.4 ± 1.8	n.d.
pyrene	243 ± 45	n.d.	463 ± 26	n.d.	8.1 ± 1.2	n.d.
2,3-*cd*]pyrene	346 ± 29	n.d.	601 ± 56	n.d.	4.8 ± 0.7	n.d.

a,h]anthracene	102 ± 7.8	n.d.	159 ± 16	n.d.	2.65 ± 0.04	n.d.
i]perylene	378 ± 52	n.d.	682 ± 86	n.d.	15.8 ± 1.2	n.d.
	115 ± 2.1	n.d.	186 ± 16	n.d.	n.d.	n.d.
US-EPA PAHs	**3400 ± 604**	**1500 ± 11**	**6900 ± 236**	**591 ± 93**	**910 ± 65**	**43 ± 9.1**
PAHs/Total PAHs	**0.49**	**0.96**	**0.54**	**1**	**0.92**	**1**

<Table>Table 3**.** Estimated yields of products released by Py-GC-MS of biochar samples, the mass to charge ratio (*m/z*) of the quantitation ion and their predominant origin: C, charred biomass; H, hemi/cellulose; L, lignin; P, proteins (nitrogen-containing compounds). Mean values ± s.d. (n = 2).

Sample Id.			**BW340**	**BW600**	**PW400**	**PW600**	**CD400**	
luct	*m/z*	origin	**µg $g_{biochar}^{-1}$**					
	78	C	172000 ± 3400	341 ± 83	265000 ± 39000	109 ± 6.8	231 ± 16	
	96	H	295 ± 52	n.d.	17.2 ± 1.5	n.d.	n.d.	
	67	P	n.d.	n.d.	30 ± 18	n.d.	n.d.	
	91	C	356000 ± 11000	38 ± 9.5	544300 ± 61500	34 ± 5.6	37.8 ± 3.3	
	95	H	53 ± 20	n.d.	n.d.	n.d.	n.d.	
	91	C	345 ± 36	3.9 ± 1.1	51.4 ± 4.2	6.3 ± 1.4	2.93 ± 0.52	
	91	C	123000 ± 3800	3.7 ± 0.2	183800 ± 16900	4.8 ± 1.2	3.87 ± 0.78	
	104	C	315 ± 34	22.8 ± 1.1	51.4 ± 1.9	7.9 ± 0.7	27.2 ± 10	
	91	C	29.7 ± 2.5	n.d.	n.d.	n.d.	n.d.	
	94	L	402000 ± 7100	n.d.	662300 ± 470700	n.d.	n.d.	
	118	C	500 ± 24	n.d.	79.1 ± 2.5	5.5 ± 0.6	n.d.	
	103	C	n.d.	n.d.	n.d.	0.90 ± 0.14	90 ± 35	
	117	P	38 ± 5.3	2.4 ± 0.3	4.8 ± 0.2	0.39 ± 0.02	2.4 ± 1.3	
	108	L	164000 ± 1500	n.d.	279100 ± 86700	n.d.	7.0 ± 1.0	
	107	L	278000 ± 37800	n.d.	497000 ± 265000	n.d.	10.5 ± 1.4	
	109	L	593 ± 73	n.d.	81.3 ± 1.2	n.d.	n.d.	
s (3 isomers)	132	C	717 ± 35	n.d.	19.3 ± 1.7	0.34 ± 0.08	n.d.	
	122	L	112000 ± 16000	n.d.	220900 ± 8860	n.d.	7.5 ± 1.4	
	128	C	42 ± 3.9	63 ± 8.7	50.4 ± 9.3	15.5 ± 0.05	193 ± 83	
	110	L	155000 ± 1600	n.d.	129 ± 13.1	n.d.	n.d.	
ne	142	C	198 ± 9.3	5.2 ± 0.8	31.9 ± 8.5	1.60 ± 0.03	36 ± 14	
ne	142	C	100 ± 4.0	5.6 ± 0.4	17.0 ± 5.6	1.92 ± 0.07	24 ± 8.6	
	138	L	386 ± 130	n.d.	2.3 ± 0.2	n.d.	n.d.	
	150	L	18 ± 2.6	n.d.	125 ± 31.6	n.d.	n.d.	
	154	C	17 ± 1.9	8.7 ± 1.1	4.1 ± 1.6	1.53 ± 0.09	11 ± 4.3	
	137	L	381 ± 99	n.d.	31.9 ± 11.7	n.d.	n.d.	
	164	C	36 ± 2.6	2.4 ± 0.12	3.1 ± 0.5	n.d.	2.30 ± 0.12	
	178	C	6.4 ± 1.2	2.5 ± 0.05	6.2 ± 0.8	n.d.	0.61 ± 0.05	
	178	C	4.66 ± 0.07	2.4 ± 0.20	1.3 ± 0.2	n.d.	n.d.	
	202	C	1.4 ± 0.2	n.d.	0.9 ± 0.1	n.d.	n.d.	
	202	C	1.3 ± 0.2	n.d.	0.7 ± 0.1	n.d.	n.d.	
)			1,770,000 ± 57,500	500 ± 100	2,650,000 ± 952,000	192 ± 16	720 ± 250	
			37	99	37	99	96	

<Table>Table 4**.** Methyl/parent PAH ratios from HyPy and Py-GC-MS (MeNap: Methylnaphthalene, Nap: naphthalene, MePhe: Methylphenanthrene, Phe; phenanthrene, MePyr: Methylpyrene Pyr: pyrene).

	HyPy		**Py-GC-MS**
Biochar	**MePhe/Phe**	**MePyr/Pyr**	**MeNap/Nap**
BW340	1.0	1.0	0.92

BW600	0.16	0.20	0.17
PW400	0.62	0.71	0.91
PW600	0.15	0.15	0.22
CD400	0.22	0.20	0.31
CD600	0.0	0.0	0.26

TDENDOFDOCTD